

Design and Control Method of a Battery/Ultra-Capacitor Energy Storage System for EVs

Fu-Sheng Pai

Department of Electrical Engineering, National University of Tainan, Tainan, Taiwan

Email: fspai@mail.nutn.edu.tw

Abstract—This paper presents a battery/ultra-capacitor (UC) energy storage system for the operation of permanent magnet synchronous motor drives in electric vehicles (EVs). In this system, when the EV is used for accelerated operation, the battery provides a stable voltage to the inverter through the DC-DC converter. At the same time, the battery and UC jointly release energy to the inverter to share the larger current demand of the EV motor. In constant speed operation, the battery supplies energy to the inverter through a shunt diode to avoid additional power losses while the DC-DC converter is operating. During the regenerative braking mode, the current produced by the EV motor is charged to the UC to reduce pulse currents flowing into the battery, which may shorten battery life. To validate the effectiveness of the circuit design, several operation scenarios including buck and boost voltage conversion for the operation of proposed battery/UC ESS were examined in the experimental studies. Test results consolidates the feasibility and practicality of the circuit method for the EV applications.

Index Terms—Energy storage system, Lithium battery, ultra-capacitor

I. INTRODUCTION

Energy storage system (ESS) is critical to electric vehicle technology, which currently consists of lithium batteries. Lithium batteries are widely adopted due to their high energy density, low self-discharge rate, and no memory effect [1–3]. Although lithium batteries have many of the above advantages, if lithium batteries are frequently charged and discharged, the cycle life of the battery will be significantly reduced. At the same time, lithium batteries are expensive. Battery failures mean that system maintenance costs will increase, hindering the development of practical applications [3–7].

To overcome the shortcomings of batteries, the UC become a viable option [7]. The UC can be charged and discharged frequently with large currents. Therefore, the use of battery and UC to form a dual-input ESS, and then using this system to improve the life cycle of EV batteries is very important today [7–9]. Over the past decade, several studies have been conducted to develop optimal circuit configurations of battery/UC dual-input energy system. As shown in Fig. 1 (a), the most common type of such a system connects the UC to the battery via a bidirectional DC-DC converter. The battery and inverter

are then cascaded to power the PMSM in EVs. In this configuration, the voltage across the UC can be used over a wide range [10]. However, the disadvantage of this circuit configuration is that the energy release or storage efficiency of the UC can be affected by the operation of the DC-DC converter. Then, a series/parallel converter-based dual-input ESS configuration is proposed, through which the charging and discharging of the battery/UC can be controlled. Fig. 1 (b) and Fig. 1 (c) show the cascaded configuration and multi-input converter configuration [11–14]. These two configurations can realize the control of battery and UC charge and discharge current, and the voltage range can also be very wide. These approaches seem feasible, but the large heat losses through multi-stage power conversion may degrade the system efficiency. Other advanced control strategies have been recently investigated for the ESS, including the model predictive control, which features online optimization, fast dynamic response, and easy constraint incorporation [15–20]. However, the predictive control-based methods with the state-space models of the system require a large number of multiplication steps, thereby complicating the circuits and system design as a whole.

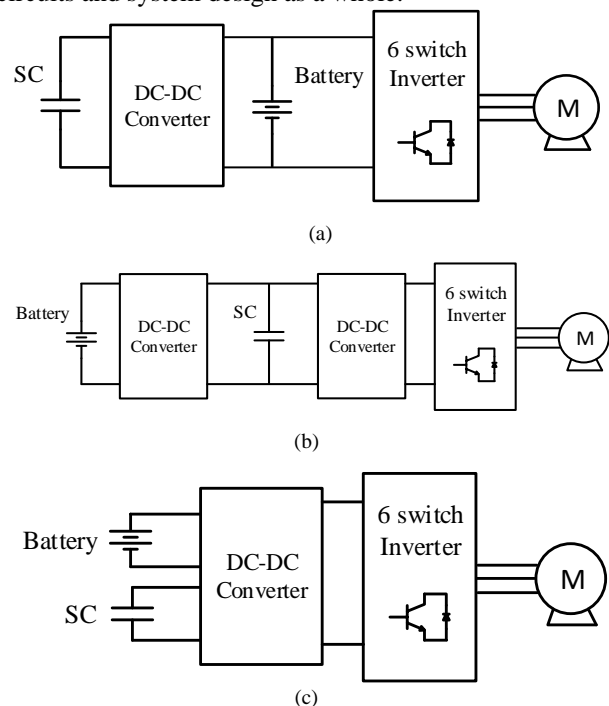


Fig. 1. Battery/ UC ESS configuration: (a) Battery/UC configuration, (b) cascaded configuration, and (c) multi-input converter configuration.

Manuscript received November 10, 2022; revised January 30, 2023; accepted March 25, 2023.

In this paper, a circuit configuration and control method for battery/UC ESS is proposed, in which an interleaved DC-DC converter is designed in the proposed circuit. Due to the torque proportional to motor current, the DC-DC converter can boost the DC bus voltage in the constant torque region to provide greater motor current for enhanced performance during acceleration. In addition, when the motor is running in constant speed mode, the battery can directly supply energy to the inverter through the anti-parallel diode inside the power switch. Using this method, the efficiency of the proposed PMSM drive can be improved by reducing the switching time of the power switch.

II. PROPOSED SYSTEM CONFIGURATION AND OPERATION

Fig. 2 (a) plots the schematic of the battery and UC ESS for PMSM drive in EVs. As shown, the system consists of battery, DC-DC converter, UC, inverter and PMSM with field oriented control as its control method. The DC-DC converter used in the proposed ESS consists of an input voltage source, two inductors, four power MOSFETs. These components can form two boost/buck converters with interleaved switches. When the vehicle is operating in the driving mode, the energy required for the PM is provided from the proposed ESS; when the vehicle is braking, the PM can be regarded as a generator, and generate the back electromotive force. The energy is recharged to the ESS as an AC power source. In the other word, the proposed ESS is a bridge between the energy storage unit and the motor of EVs, which is able to distribute the energy flow direction by switching the power MOSFET components correctly.

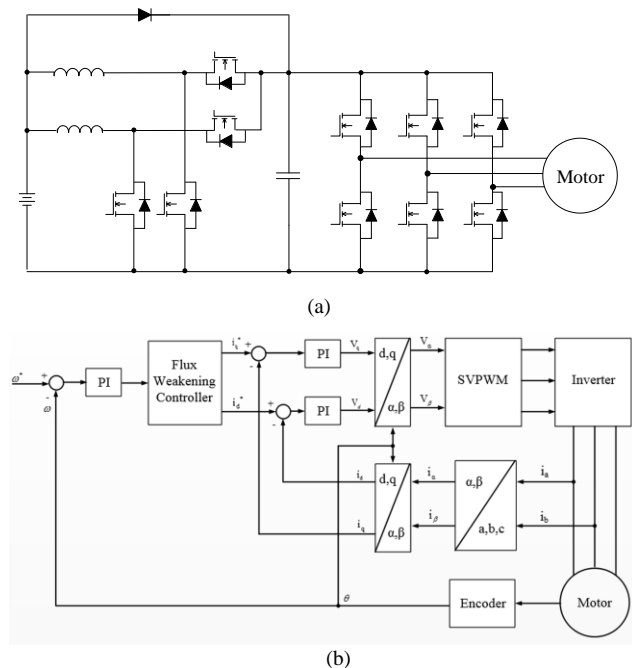


Fig. 2. Schematic diagram of the proposed HESS for a PMSM drive: (a) Main Power Stage and (b) Control block diagram of FOC for a PMSM.

In the circuit, when the system starts up, the battery energy supplies power to the UC through a DC-DC converter, which builds the proper DC voltage across the UC. Next, an inverter is employed to control the speed and torque of the motor. As shown in Fig. 2 (b), an SVPWM-based circuit related to the outer speed and inner current loop is used to control the power switch to supply the load current. These two loops are coordinated inside the controller, where the speed loop is the first loop of the controller to keep the motor speed at the desired value and its output signal is fed to the inner loop so that the desired gating signals are generated for power switches. With such a control scheme, Park, Inverse Park, Clarke, and Inverse Clarke transforms are used to decouple the torque and flux signals for field-oriented control. It is beneficial to the drive circuit to obtain better linear motor control effect.

In addition, due to the limitation of the inverter circuit, high torque and high speed cannot be achieved at the same time. Under these system constraints, the proposed ESS can switch circuit modes according to different operating conditions.

- 1) The acceleration mode: In this mode, high current is required for high torque. Therefore, both the battery and the UC need to provide motor current. As shown in Fig. 3 (a), in the acceleration mode, the battery voltage is boosted by the DC-DC converter to obtain a higher DC-bus voltage, and then the battery and UC are combined to provide the energy required by the motor.
- 2) The constant speed mode: As shown in Fig. 3 (b), the motor only needs a small current to keep running at a constant speed. In this case it is sufficient to use only capacitors. Therefore, UC is used to supply all load currents. DC-DC is temporarily turned off to reduce circuit losses. However, when the UC voltage drops below the battery voltage, the battery can supply energy to the inverter through the shunt diode D_{sh} .
- 3) The regenerative braking mode: In this mode, the kinetic energy of the vehicle is fed back to the proposed ESS. As shown in Fig. 3 (c) and 3 (d), if the UC can work normally, the regenerative energy of the PMSM will be stored in the UC, thus preventing the batteries from being rapidly charged by the regenerative pulse power. However, when the UC reaches the voltage limit, the UC has no ability to store energy and all the recovered energy will be transferred to the battery by the DC-DC converter work.

Based on the circuit configuration, Fig. 4 shows the main waveforms of the proposed DC-DC converter. In this figure, each switching cycle is divided into 8 modes. The inductor currents indicate that they operate in continuous conduction mode. Then, the two gate pairs of (Q_1, Q_2) or (Q_3, Q_4) are shifted by 180 degrees for interleaving operation. This circuit switching method reduces output voltage ripple and reduces the need for larger output capacitors in parallel.

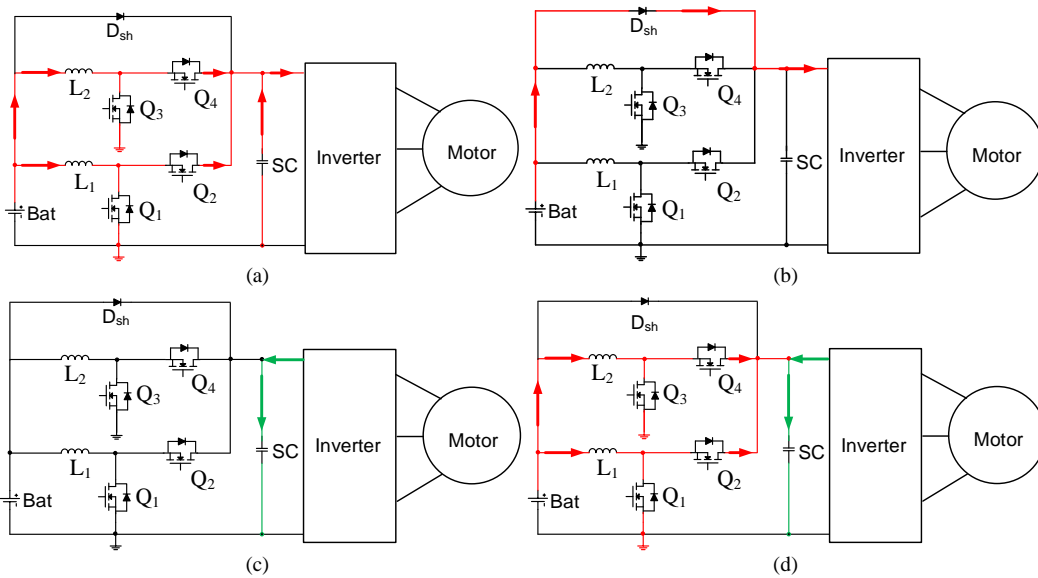


Fig. 3. Power flow of proposed HESS under different vehicle operation: (a) Motor acceleration, (b) motor constant speed, (c) regenerative braking mode (I), and (d) regenerative braking mode (II).

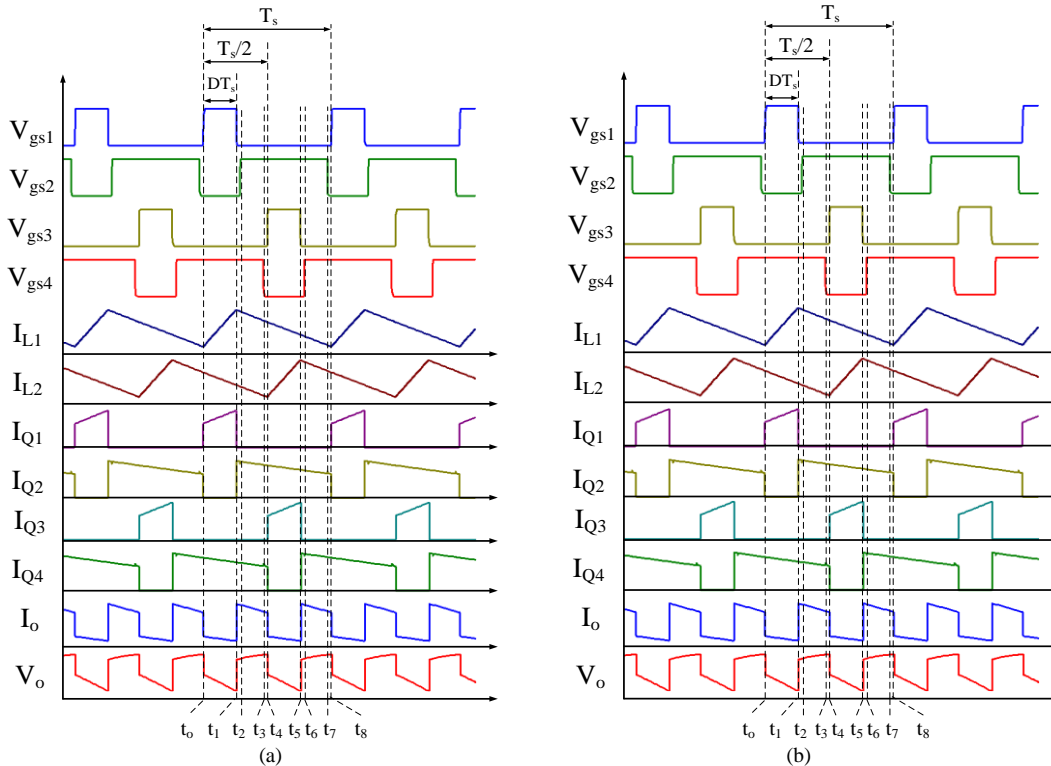


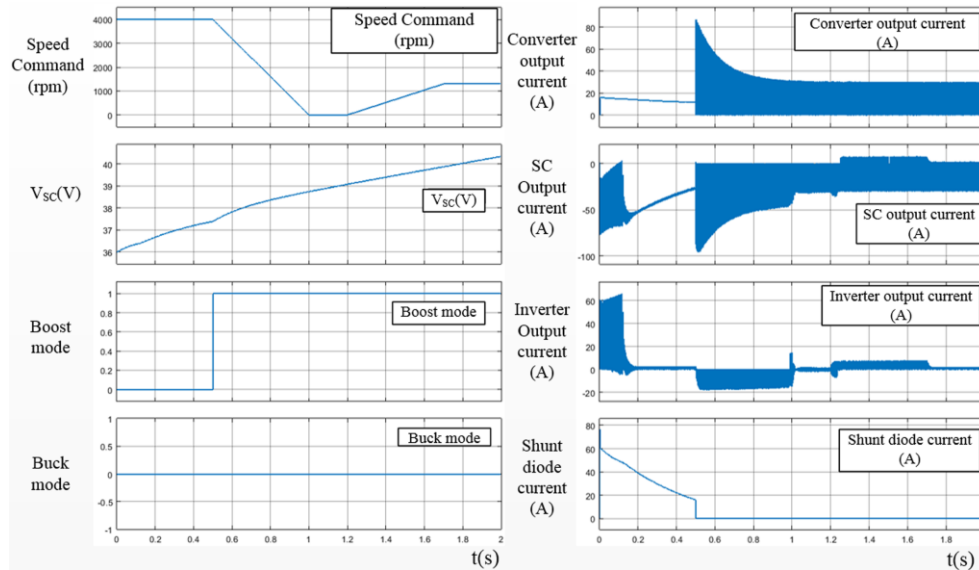
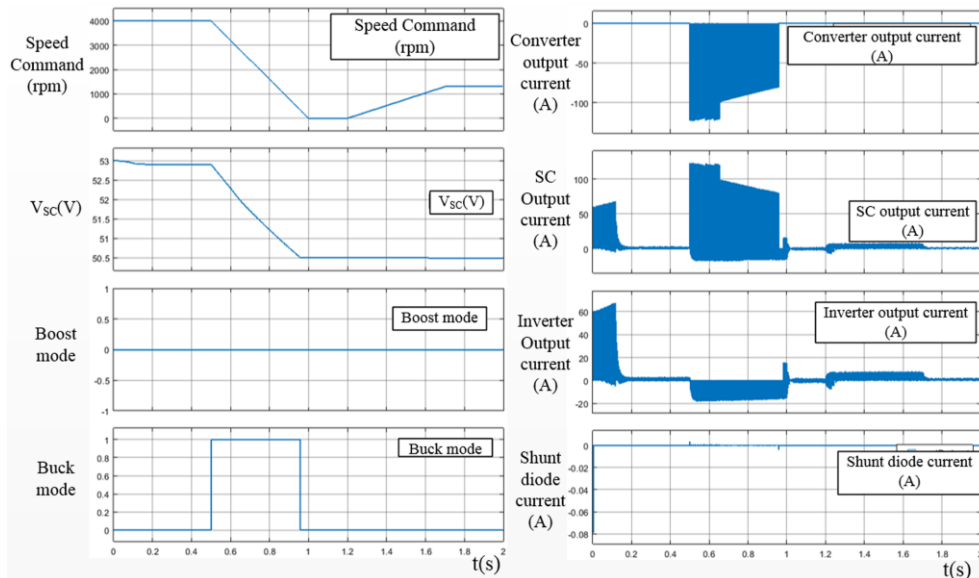
Fig. 4. Main waveforms of proposed interleaved DC-DC converter: (a) in the boost mode and (b) in the buck mode.

III. SIMULATIONS OF PROPOSED ESS WITH MOTOR DRIVE

To validate the proposed method, Fig. 2 is used as a test system to be simulated, where a 1kW ESS system is developed for the test. The battery voltage is varied between 32 V and 42 V, the allowable DC link voltage across UC, V_{uc} , is 36 V to 51 V, and the rated DC voltage of the inverter for motor control is 48 V.

Fig. 5 shows that the batteries provides energy to the motor directly through the diode D_{sh} when V_{uc} is at 36 V. In this case, V_{uc} is lower than the batteries voltage of 48 V. Because the current only flows through the shunt diode

instead of the bidirectional converter, the switching loss can be reduced and save more energy for long-term operation. In the regenerative braking mode, V_{uc} is much lower than 48 V, so the batteries charge UC through the boost converter and the motor charges UC. When the motor accelerates and the voltage across UC is lower than 48 V, the boost mode is turned on to supply energy. In low constant speed mode and V_{uc} is near 48 V, the boost mode is turned off and only the UC supply current to the motor. With UC, the charge/discharge times of the batteries are largely reduced, which can extend the batteries lifetime.


 Fig. 5. Simulation results of different operational conditions at $V_{uc}=36$ V.

 Fig. 6. Simulation results of different operational conditions at $V_{uc}=53$ V.

Next, Fig. 6 shows the simulation results of ESS with different operational conditions at V_{uc} of 53 V. In this case, because V_{uc} is higher than the maximum voltage that UC can afford, the buck mode is turned on in the regenerative braking mode to release energy and charge the batteries. When the motor is accelerating, V_{uc} is still higher than the rated voltage of 48V, only UC supplies current to the motor, which helps the batteries extend the lifetime.

IV. EXPERIMENTAL RESULTS

In order to verify the proposed method, experimental results have been compared. The test circuit is shown in Fig. 2. The experimental specifications are shown in Table I. Fig. 7 shows the main test waveforms of the proposed DC-DC converter in the boost mode. According to Fig. 7, there is a 180-degree phase shift between the two currents of the two inductors, which means that the circuit presented in this paper can indeed reduce the output ripple through the interleaved switching technique.

Furthermore, Fig. 8 shows the output waveforms of the proposed DC-DC in buck modes. In the figure, there are few voltage spikes in the drain-source voltage waveform of the power switches due to stray inductance and capacitance in the circuit. However, the inductor's current waveform is not affected because the graph depicts a linear change and operates in continuous conduction mode. In addition, the output voltage ripple is 0.45 V in boost mode and 0.08 V in buck mode, thus maintaining the power supply quality of the proposed ESS.

TABLE I: SPECIFICATIONS OF PROPOSED DC-DC CONVERTER

Battery Voltage Range	30~42 V
Nominal Battery Voltage V_{Bat}	36 V
Ultra-capacitor Voltage Range	36~51 V
Nominal Ultra-capacitor Voltage V_{uc}	48 V
Rated Output Power P_o	1 kW
Converter switching Frequency f_s	100 kHz

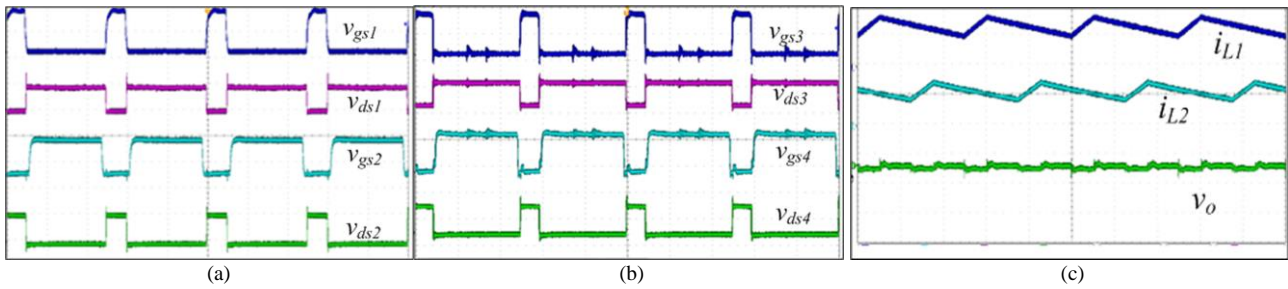


Fig. 7. Experimental results of DC-DC converter in the boost mode: (a) Gate signals and drain-source voltage of MOSFET Q1 and Q2, (b) gate signals and drain-source voltage of MOSFET Q3 and Q4, and (c) inductor current and UC voltage.

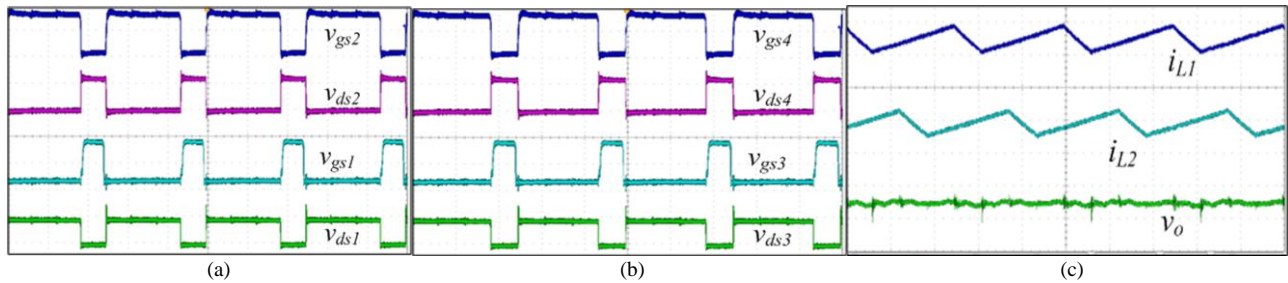


Fig. 8. Experimental results of DC-DC converter in the buck mode: (a) Gate signals and drain-source voltage of MOSFET Q1 and Q2, (b) gate signals and drain-source voltage of MOSFET Q3 and Q4, and (c) inductor current and battery voltage.

V. CONCLUSIONS AND FUTURE WORK

This paper proposes a battery and ultra-capacitor ESS for PMSM drive, which can switch between different modes according to the operating conditions of the PMSM. In this method, the DC-DC converter in the proposed ESS is only turned on in the motor acceleration and braking modes, because the large amount of heat and power loss generated by the conventional two-stage power conversion may reduce the energy conversion efficiency of the whole system. Due to the shorter operation time and higher efficiency of the DC-DC converter operation, the proposed ESS can operate in a better state. For the battery, reducing the inflow of pulse current generated by the motor braking can also avoid the problem of shortening the battery life. Currently, the circuit scheme proposed in this study is being implemented on an electric scooter. The test results will be presented in future research work.

CONFLICT OF INTEREST

The author declares no conflict of interest.

ACKNOWLEDGMENT

This work is supported by the National Science and Technology Council, Taiwan, under project MOST 111-2221-E-024 -004.

REFERENCES

- [1] M. Elmahallawy, T. Elfouly, A. Alouani, and A. M. Massoud, "A comprehensive review of lithium-Ion batteries modeling, and state of health and remaining useful lifetime prediction," *IEEE Access*, vol. 10, pp. 119040-119070, Nov. 2022.
- [2] A. Rastegarpanah, Y. Wang, and R. Stolkin, "Predicting the remaining life of lithium-ion batteries using a CNN-LSTM model," in *Proc. 8th International Conference on Mechatronics and Robotics Engineering*, Munich, 2022, pp. 73-78.
- [3] M. F. Hsieh, P. S. Chen, F. S. Pai, and R. Y. Weng, "Development of hybrid energy storage system with battery/ supercapacitor to enhance battery life cycle for EV permanent magnet synchronous motor drives," *Sustainability*, vol. 13, no. 14, pp. 7682-7695, July, 2021.
- [4] A. Alyakhni, L. Boulon, J. M. Vinassa, and O. Briat, "A comprehensive review on energy management strategies for electric vehicles considering degradation using aging models," *IEEE Access*, vol. 9, pp. 113922-113940, Oct. 2021.
- [5] Y. Gao, K. Liu, C. Zhu, X. Zhang, and D. Zhang, "Co-estimation of state-of-charge and state-of-health for lithium-ion batteries using an enhanced electrochemical model," *IEEE Trans. on Industrial Electronics*, vol. 69, no. 3, pp. 2684-2696, Mar. 2022.
- [6] X. B. Han, M. G. Ouyang, L. G. Lu, and J. Q. Li, "Cycle life of commercial lithium-ion batteries with lithium titanium oxide anodes in electric vehicles," *Energies*, vol. 7, no. 4, pp. 4895-4909, 2014.
- [7] J. Cao and A. Emadi, "A new battery/ultracapacitor hybrid energy storage system for electric, hybrid, and plug-in hybrid electric vehicles," *IEEE Trans. on Power Electronics*, vol. 27, no. 1, pp. 122-132, 2012.
- [8] H. H. Eldeeb, A. T. Elsayed, C. R. Lashway, and O. Mohammed, "Hybrid energy storage sizing and power splitting optimization for plug-in electric vehicles," *IEEE Trans. on Industry Applications*, vol. 55, no. 3, pp. 2252-2262, 2019.
- [9] J. Shen, S. Dusmez, and A. Khaligh, "Optimization of sizing and battery cycle life in battery/ultracapacitor hybrid energy storage systems for electric vehicle applications," *IEEE Trans. on Industrial Informatics*, vol. 10, no. 4, pp. 2112-2121, Nov. 2014.
- [10] L. Zhang, X. Hu, Z. Wang, F. Sun, J. Deng, and D. G. Dorrell, "Multiobjective optimal sizing of hybrid energy storage system for electric vehicles," *IEEE Trans. on Vehicular Technology*, vol. 67, no. 2, pp. 1027-1035, 2018.
- [11] M. Asensio, G. A. Magallan, E. G. Amaya, and C. H. De Angelo, "Efficiency and performance analysis of battery-ultracapacitor based semi-active hybrid energy systems for electric vehicles," *IEEE Latin America Transactions*, vol. 16, no. 10, pp. 2581-2590, 2018.
- [12] S. M. Lukic, J. Cao, R. C. Bansal, F. Rodriguez and A. Emadi, "Energy storage systems for automotive applications," *IEEE Trans. on Industrial Electronics*, vol. 55, no. 6, pp. 2258-2267, Jun. 2008.
- [13] W. Deng, Y. Zhao, and J. Wu, "Energy efficiency improvement via bus voltage control of inverter for electric vehicles," *IEEE Trans. on Vehicular Technology*, vol. 66, no. 2, pp. 1063-1073, Feb. 2017.
- [14] A. D. Napoli, F. C. Cimbini, F. G. Capponi, and L. Solero, "Control strategy for multiple input DC-DC power converters

- devoted to hybrid vehicle propulsion systems,” in *Proc. IEEE International Symposium Industrial Electronics*, vol. 3, no. 2, May 2002, pp. 1036-1041.
- [15] F. Naseri, E. Farjah, and T. Ghanbari, “An efficient regenerative braking system based on battery/supercapacitor for electric, hybrid, and plug-in hybrid electric vehicles with BLDC motor,” *IEEE Trans. on Vehicular Technology*, vol. 66, no. 5, pp. 3724–3738, May, 2017.
- [16] W. L. Jing, C. H. Lai, S. H. W. Wong, and M. L. D. Wong, “Battery-supercapacitor hybrid energy storage system in standalone DC microgrids: a review,” *IET Renewable Power Generation*, Vol. 11, no. 4, pp. 461-469, Jan, 2017.
- [17] A. Allam and S. Onori, “Online capacity estimation for lithium-ion battery cells via an electrochemical model-based adaptive interconnected observer,” *IEEE Trans. on Control Systems Technology*, vol. 29, no. 4, pp. 1636–1651, Jul. 2021.
- [18] L. Ling and Y. Wei, “State-of-charge and state-of-health estimation for lithium-ion batteries based on dual fractional-order extended kalman filter and online parameter identification,” *IEEE Access*, vol. 9, pp. 47588–47602, Mar. 2021.
- [19] U. Manandhar, N. R. Tummuru, S. K. Kollimalla, A. Ukil, G. H. Beng, and K. Chaudhari, “Validation of faster joint control strategy for battery- and supercapacitor-based energy storage system,” *IEEE Trans. on Industrial Electronics*, vol. 65, pp. 3286–3295, Sept. 2018.
- [20] X. Zhang, Y. Han, and W. Zhang, “A review of factors affecting the lifespan of lithium-ion battery and its health estimation methods,” *Transactions on Electrical and Electronic Materials*, vol. 22, pp. 567–574, Jul. 2021.

Copyright © 2023 by the authors. This is an open access article distributed under the Creative Commons Attribution License (CC BY-NC-ND 4.0), which permits use, distribution and reproduction in any medium, provided that the article is properly cited, the use is non-commercial and no modifications or adaptations are made.



Fu-Sheng Pai received the Ph.D. degree in Department of Electrical Engineering from National Cheng Kung University, Tainan, Taiwan, in 2002. He is Professor with Department of Electrical Engineering, National University of Tainan, Taiwan. He has worked on projects at the Delta Electronics, Inc from 1999 to 2002. His current areas of interests are power electronics circuit design, system analysis, and industry applications.